Parallel Orthogonalization Techniques

Julian Schmitt
Institute of Mathematics
EPFL
Lausanne, Switzerland

Abstract

We study and compare three algorithms (classical Gram-Schmidt, modified Gram-Schmidt and Tall Skinny QR) for the orthogonalization of a set of vectors. The goal is to identify a method that is numerically stable and scales well in parallel.

1 Introduction

In this project, we study the following three algorithms for the orthogonalization of a set of vectors: Classical Gram-Schmidt (CGS), Modified Gram-Schmidt (MGS) and the Tall Skinny QR (TSQR) decomposition. In particular, we aim to find efficient parallelized implementations in order to retrieve the thin QR factorization of a given matrix $W \in \mathbb{R}^{m \times n}$. Key aspects of our research are numerical stability, orthogonality of the computed basis $Q \in \mathbb{R}^{m \times n}$, scalability and performance compared to the corresponding sequential algorithms.

For the parallelization, we use a block row distribution - one block per processor. The numerical stability will be analyzed by measuring the loss of orthogonality $||I - Q^T Q||_2$ and the condition $\kappa(Q)$ of the orthonormal basis Q. In particular, we confirm theoretical bounds on the loss of orthogonality provided by [5]. For our numerical experiments, we use (among others) the following four matrices W^1, W^2, W^3 and W^4.

The first matrix $W^1 \in \mathbb{R}^{m \times n}$ is generated by uniformly discretizing the parametric function

$$f(x, \mu) = \frac{\sin(10(\mu + x))}{\cos(100(\mu - x)) + 1.1}, \quad 0 \leq x, \mu \leq 1.$$

W^1 is then defined as $W^1_{i,j} = f(\frac{i-1}{m-1}, \frac{j-1}{n-1})$ with $i \in [m]$, $j \in [n]$ and was originally introduced in [1]. As matrix dimensions we choose $m = 50000$ and $n = 600$. The condition of W^1 is $\kappa(W^1) = 6.18 \cdot 10^{15}$.

The second matrix W^2 is the so-called "abtaha2"-matrix from the SuiteSparse Matrix Collection [3]. This matrix is based on a combinatorial optimization problem and it is therefore an integer matrix $W^2 \in \mathbb{Z}^{37932 \times 331}$. Nevertheless, the matrix is well suited for testing our parallelizations because of its "tall and skinny" shape. Its condition is $\kappa(W^2) = 12.2$ and therefore we use it as a reference for matrices with a small condition.

Although our algorithms are designed for input matrices with $m \gg n$, it will be interesting to see how they perform on square matrices. For this purpose, we chose the well-known Hilbert matrix as $W^3 \in \mathbb{R}^{1000 \times 1000}$. As a classical example of ill-conditioned matrices and $\kappa(W^3) = 3.14 \cdot 10^{20}$ being even greater than $\kappa(W^1)$, it will be of special interest for our research on numerical stability. However, we will not be able to execute TSQR on this matrix (details see later).

The last matrix $W^4 \in \mathbb{R}^{4472 \times 936}$ with the name "photogrammetry2" is again chosen from the SuiteSparse Matrix Collection [3]. It originally arose from a computer vision problem and has an intermediate condition (compared to the other three matrices) of $\kappa(W^4) = 1.34 \cdot 10^8$. The matrix serves as another example of naturally occurring matrices.

Preprint. Under review.

Algorithm 1 Sequential CGS

```
1: for $i = 1$ to $n$ do
2:     if $i > 1$ then
3:         $R[1:i-1, i] = W[:, 1:i-1]^T \, W[:, i]$
4:         $W[:, i] = W[:, i] - W[:, 1:i-1] \, R[1:i-1, i]$
5:     end if
6:     $R[i, i] = || \, W[:, i] \, ||_2$
7:     $W[:, i] = W[:, i] \; / \; R[i, i]$
8: end for
9: return $W, R$
```

1.1 About Numerical Experiments

For the numerical analysis and performance evaluation we executed all algorithms on a single machine with an Intel Core i5 6500 (4×3.6 GHz, 6MB L3 cache) processor and 16 GB of DDR4-RAM powered by Fedora 38 (64-Bit, Linux Kernel 6.5.6). Furthermore, the algorithms have been implemented in Python 3.11.5 using NumPy 1.26.0. The parallelization has been done via the Python implementation *mpi4py* (Version: 3.1.4) of the well-known Message Passing Interface (MPI) (OpenMPI 4.1.4).

NumPy uses an underlying BLAS (Basic Linear Algebra Subprograms) library for matrix-matrix and matrix-vector products. These BLAS routines are multi-threaded by default. Since we want to compare runtimes of sequential and parallel versions of CGS, MGS and TSQR on a single machine, we disable this multi-threading by limiting the threads available for BLAS operations to 1. This can be achieved by setting the environment variable *OMP_NUM_THREADS* accordingly.

Finally, throughout this report, we will refer to the machine precision as u. On our system it holds $u = 2.220446049250313 \cdot 10^{-16}$ for the type *float* (or *single precision*).

2 Classical Gram-Schmidt (CGS)

The Classical Gram-Schmidt algorithm is a method for orthonormalizing a set of vectors. Given vectors $w_1, ..., w_n$ as columns of the input matrix W, the Gram-Schmidt process iteratively computes the corresponding orthonormal basis $q_1, ..., q_n$ as follows:

$$q'_k = w_k - \sum_{i=1}^{k-1} \langle q_i, w_k \rangle \qquad q_k = \frac{q'_k}{||q'_k||_2} \qquad \forall k \in [n] \tag{1}$$

$q_1, ..., q_n$ are the columns of the matrix Q of the QR decomposition of W. The matrix R can be obtained either by computing $R = Q^T W$ at the end or already while computing the orthonormal basis Q as in Algorithm 1. In the pseudo-code we use a Python like notation to represent submatrices. In order to exploit highly optimized BLAS-routines, we work only with vectors and matrices instead of scalars. Note, Algorithm 1 is the *left-looking* variant of CGS and is dominated by Level-2-BLAS operations since it only uses (dense) matrix-vector and no matrix-matrix products. Finally, it is worth mentioning that the matrix Q is computed *in-place* to improve memory usage. Overall, the algorithm requires $2mn^2$ floating-point operations.

2.1 Parallelization of CGS

A problem when parallelizing CGS using a row distribution of processors is the computation of the norm and dot products of each column vector w_k with the former vectors $q_1, ..., q_{k-1}$. This calculation has to be done by synchronizing all processors, accumulating local dot products and making the final result known globally.

Algorithm 2 is the parallelized version of Algorithm 1. We use two *allreduce* operations per iteration and accordingly, the number of messages across the processors scales linear with the number of columns of the input matrix W. It holds $\#$ *messages* $\doteq 4n \log(P)$ (lower-order terms omitted). It is worth mentioning that there is a lower bound of $2n \log(P)$ messages for the (left-looking) CGS [4]. Therefore, our algorithm could be improved to use only half of the amount of messages. Algorithm

Algorithm 2 Parallel CGS

```
1: MPI.ScatterV(W, B, root = 0)
2: for $i = 1$ to $n$ do
3:     if $i > 1$ then
4:         $R[1:i-1, i] =$ MPI.ALLREDUCE($B[:, 1:i-1]^T\ B[:, i]$, MPI.SUM, root $= 0$)
5:         $B[:, i] = B[:, i] - B[:, 1:i-1] \cdot R[1:i-1, i]$
6:     end if
7:     $q =$ MPI.ALLREDUCE($B[:, i]^T B[:, i]$, MPI.SUM, root $= 0$)
8:     $R[i, i] = \sqrt{q}$
9:     $B[:, i] = B[:, i] / R[i, i]$
10: end for
11: MPI.GatherV($B$, $W$, root = 0)
12: return $W, R$
```

Figure 1: Runtime of sequential and parallel CGS

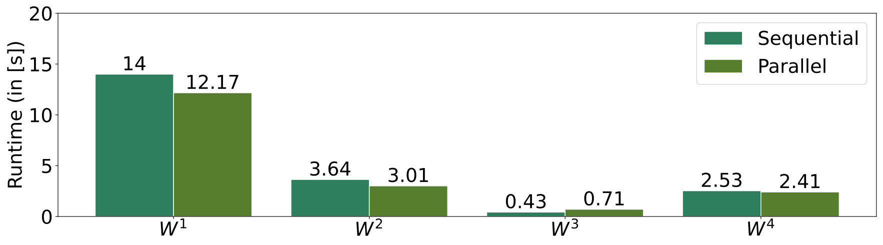

2 first scatters the matrix $W \in \mathbb{R}^{m \times n}$ into row-blocks $B \in \mathbb{R}^{\frac{m}{P} \times n}$ - one for each processor. Then, each processor iterates over the columns of its block B. $R[1:i-1, i]$ is computed by calculating $B[:, 1:i-1]^T B[:, i]$ locally and accumulating the result globally. After that $B[:, i]$ can be computed by each processor independently. Finally, to normalize $B[:, i]$ and retrieve $R[i, i]$ we have to compute the norm $||\ W[:, i]\ ||_2$ through another reduce operation on local dot products. Since we computed again in-place (as in Algorithm 1), the matrix Q is retrieved by gathering the local matrices B together. Note that the matrix R is computed and stored by each processor redundantly because it is a by-product of calculations necessary for Q. Of course, one can easily modify the algorithm to store R only on one processor.

2.2 Performance Evaluation of CGS

In this subsection, we want to compare the runtimes of Algorithms 1 and 2. As mentioned in the introduction, the number of threads available to BLAS has been limited by setting OMP_NUM_THREADS $= 1$. Furthermore, we explicitly computed the Q and R matrix in both algorithms and used all 4 available processors for the parallel algorithm. Figure 1 shows the average runtimes of 10 code executions. From the bar plot we can see that parallel CGS does indeed perform better than sequential CGS. However, this effect is only useful for large and rectangular matrices. For example, for the small quadratic matrix W^3 the communication overhead is so large that the sequential algorithm outperforms the parallelized version.

2.3 Numerical Stability of CGS

CGS is in general said to be numerical unstable. The orthogonal projections of the columns of W are affected by rounding errors which accumulate for an increasing column number n. In contrast to the Modified Gram-Schmidt algorithm which will be discussed in the next section, CGS does not correct errors from previous steps.

Grigori [5] gives the following theoretical bound on the loss of orthogonality: Assuming $c_1(m,n)\kappa^2(W)u < 1$, it holds $||I - Q^TQ||_2 = c_2(m,n)\kappa^2(W)u$ with $c_1(m,n), c_2(m,n) = O(mn^2)$. In particular, the loss of orthogonality scales quadratic with the condition $\kappa(W)$. In Table 1 we present the orthogonality loss as well as $\kappa(Q)$ of sequential and parallel CGS (Algorithms 1 and 2) for our four test matrices. Nevertheless, our test matrices are not well-suited to demonstrate that our algorithms match $||I - Q^TQ||_2 = O(\kappa^2(W)u)$ because they vary in size and condition at the same

Table 1: Orthogonality loss $||I - Q^TQ||_2$ of CGS

Algorithm	$\mathbf{W}^1$		$\mathbf{W}^2$		$\mathbf{W}^3$		$\mathbf{W}^4$	
	loss	$\kappa(Q)$	loss	$\kappa(Q)$	loss	$\kappa(Q)$	loss	$\kappa(Q)$
Sequential	352.4	$6.5 \cdot 10^{16}$	$2.9 \cdot 10^{-14}$	1	992.7	$2.2 \cdot 10^{22}$	3.4	$16 \cdot 10^4$
Parallel	408.5	$7.7 \cdot 10^{16}$	$4.2 \cdot 10^{-14}$	1	992.3	$3 \cdot 10^{20}$	3.5	$3.5 \cdot 10^4$

Figure 2: CGS - Orthogonality loss and $\kappa(Q)$ as function of $\kappa(W)$

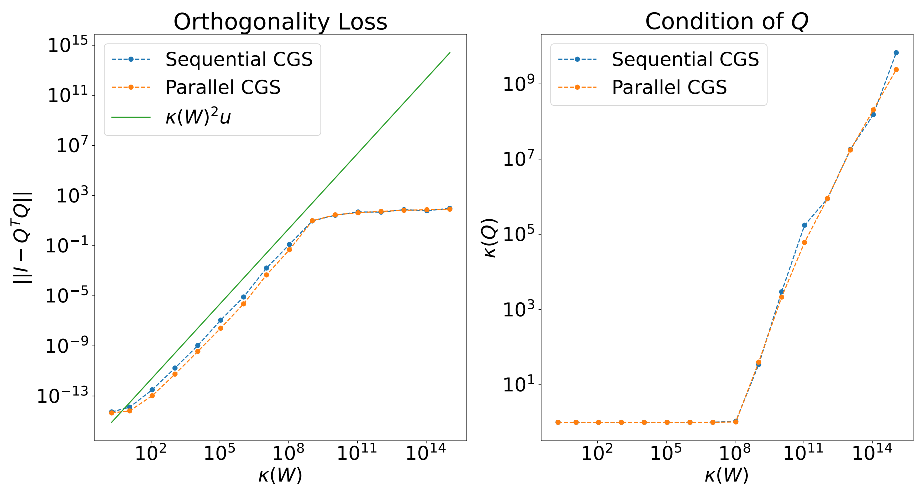

time. For this reason, we introduce a procedure presented in [7] to generate matrices $W \in \mathbb{R}^{m\times n}$ with condition number ranging from 1 to 10^{15} and having the same size: We set $W = UDV^T$ where $U \in \mathbb{R}^{m\times n}$ and $V \in \mathbb{R}^{n\times n}$ are obtained by computing the QR factorization of normally distributed random matrices. The diagonal matrix $D \in \mathbb{R}^{n\times n}$ has the following elements

$$D = \text{diag}(d_1, \dots, d_n), \quad d_i = 10^{\alpha(i-1)}, \quad \alpha = \frac{\log_{10}\kappa(W)}{m-1}.$$

As matrix dimensions, we chose $m = 2000$ and $n = 200$. By varying the value of $\kappa(W)$ we obtain a sequence of matrices with the desired conditions in $[1, 10^{15}]$.

Figure 2 shows the orthogonality loss as well as the condition of the orthonormal basis Q of sequential and parallel CGS (Algorithms 1 and 2) for these test matrices. The green line in the plot on the left illustrates $\kappa^2(W)u$ as a reference. For $\kappa(W) \leq 10^9$ both algorithms perfectly match the theoretical prediction and for $\kappa(W) > 10^9$ they perform even better. One reason for the mismatch might be that the bound given by [5] holds only for $c_1(m,n)\kappa^2(W)u < 1$. Moreover, the same phenomenon could be observed in [7]. In the plot on the right, we can see that $\kappa(Q)$ is strongly dependent on $\kappa(W)$. Finally, note that as expected sequential and parallel CGS produce almost the same results.

In order to investigate the evolution of the orthogonality error $||I - Q^TQ||_2$ and the condition of the orthonormal basis Q, we measured both in each iteration of the CGS algorithms. Figure 3 illustrates our results for W^1, W^2, W^3, W^4. The lines corresponding to each matrix stop at different iterations because they differ in the number of columns. Once again, both algorithms behave quite similarly. While the orthogonality errors of W^1, W^2 are at a very high level from the first iterations onwards, the error of W^4 jumps only in the last iterations. As expected, for the well-conditioned matrix W^2 the orthogonality error and condition of Q stay very small. Finally, note that for all matrices $\kappa(Q)$ is at a similar level as $\kappa(W)$ throughout the iterations.

3 Modified Gram-Schmidt (MGS)

The Modified Gram-Schmidt algorithm is mathematically equivalent to the previously presented Classical Gram-Schmidt method. However, the involved matrix-vector operations are rearranged in order to improve numerical stability and avoid round-off errors. The MGS constructs an orthogonal

Figure 3: Numerical Analysis of CGS

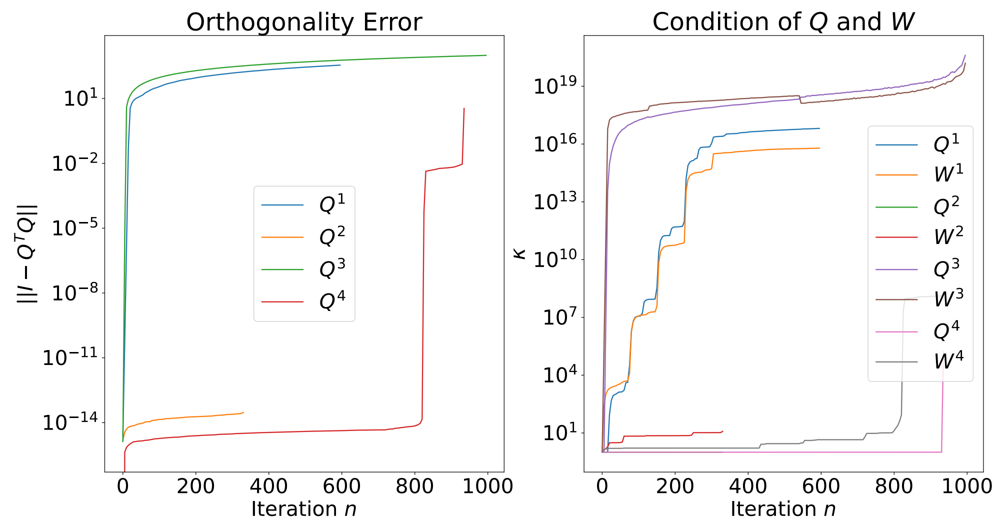

(a) Sequential CGS

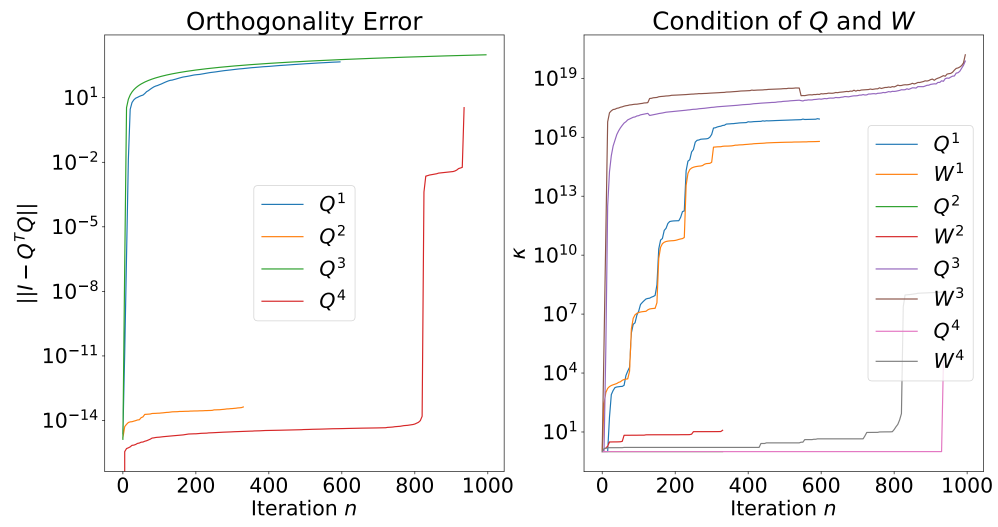

(b) Parallel CGS

set of vectors from the columns of the given matrix W through an iterative process of modifying all forthcoming vectors to be orthogonal to the already computed ones. In particular, in each step vectors are orthogonalized based on the previous orthogonalization. This is the major difference compared to CGS and allows correcting for rounding errors. The i-th iteration of the MGS is:

$$\begin{aligned} r_{ij} &:= \frac{w_i^T w_j}{||w_i||_2} && \forall j \in \{i, \dots, n\} \\ q_j &:= w_j - r_{ij} w_i && \forall j \in \{i+1, \dots, n\} \\ q_i &:= \frac{w_i}{r_{ii}} \end{aligned} \tag{2}$$

where w_i is the i-th column of W. The matrix $R \in \mathbb{R}^{n \times n}$ of the QR decomposition can be retrieved by the corresponding multipliers r_{ij}. The pseudo-code for the sequential MGS can be found in Algorithm 3. Similar to the implementation of CGS, the algorithm works in-place and therefore the matrix Q is stored within W. Again, we work only with vectors and matrices instead of scalars to

Algorithm 3 Sequential MGS

```
1: for $i = 1$ to $n$ do
2:     $R[i,i] = ||\, W[:,i]\, ||_2$
3:     $W[:,i] = W[:,i]/R[i,i]$
4:     if $i < n$ then
5:         $R[i,i+1:n] = W[:,i]^T W[:,i+1:n]$
6:         $W[:,i+1:n] = W[:,i+1:n] - W[:,i]R[i,i+1:n]^T$
7:     end if
8: end for
9: return $W, R$
```

Algorithm 4 Parallelized MGS

```
1: MPI.SCATTERV($W$, $B$, root = 0)
2: for $i = 1$ to $n$ do
3:     $v = B[:,i]^T B[:,i:n]$
4:     $v$ = MPI.REDUCE($v$, MPI.SUM, root = 0)
5:     if rank == 0 then
6:         $v = v/\sqrt{v[1]}$
7:     end if
8:     $v$ = MPI.BCAST($v$, root = 0)
9:     $B[:,i] = B[:,i] \,/\, v[1]$
10:    $R[i,i:n] = v$
11:    $B[:,i+1:n] = B[:,i+1:n] - B[:,i]\; R[i,i+1:n]$
12: end for
13: MPI.GATHERV($B$, $W$, root = 0)
14: return $W, R$
```

exploit the BLAS-routines. Note, Algorithm 3 is the *right-looking* variant of MGS and exclusively matrix-vector operations are used. Therefore only Level-2 BLAS routines can be leveraged. However, there are indeed more complex reformulations of MGS that use CGS as a subroutine to access Level-3 BLAS routines [6]. As the algorithm for CGS, Algorithm 3 requires $2mn^2$ floating-point operations. Nevertheless, the concept of modifying all forthcoming vectors in each iteration causes additional overhead and therefore MGS is not as efficient as CGS.

3.1 Parallelization of MGS

As for the CGS, the main problem when parallelizing MGS is the computation of the norm of each vector and its inner product with subsequent vectors. Since we use a row distribution for parallelization, a process of accumulating the inner products across processors and making these known globally is necessary.

In Algorithm 4 we managed to reduce the communication across processors to a *reduce* and a *broadcast* operation per iteration. Therefore, we have # messages $\doteq 2n\log(P)$ and this is indeed the lower bound for the number of messages for (right-looking) MGS [4]. Recall that this is only half of the number of messages we needed for the parallelized CGS. To achieve this, Algorithm 4 reorders the operations of Algorithm 3. First of all, row-blocks $B \in \mathbb{R}^{\frac{m}{P}\times n}$ of the matrix $W \in \mathbb{R}^{m\times n}$ are scattered across the available processors P. After that, each processor iterates over the columns of its local block B. The algorithm computes $R[i,i:n] = (W[:,i]^T W[:,i+1:n])/||W[:,i]||_2$ by calculating $B[:,i]^T B[:,i:n]$ locally, then summing those vectors across processors via a reduce and finally broadcasting the normed vector back. The rest of the computation can be done locally. The final matrix Q stored in W must be retrieved by gathering all local blocks back together. Note that the matrix R is computed and stored by each processor redundantly.

3.2 Performance Evaluation of MGS

Now, let us compare the performance of the parallelized and the sequential MGS. Figure 4 shows the runtime of Algorithms 3 and 4 computing the QR decomposition of our four test matrices. Again,

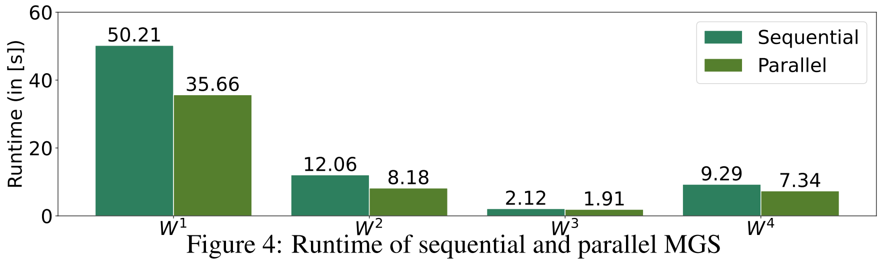

Figure 4: Runtime of sequential and parallel MGS

Table 2: Orthogonality loss $||I - Q^TQ||_2$ of MGS

Algorithm	$\mathbf{W}^1$		$\mathbf{W}^2$		$\mathbf{W}^3$		$\mathbf{W}^4$	
	loss	$\kappa(Q)$	loss	$\kappa(Q)$	loss	$\kappa(Q)$	loss	$\kappa(Q)$
Sequential	9.95	9.54	$4.05 \cdot 10^{-14}$	1	8.01	21664.67	$2.82 \cdot 10^{-8}$	1
Parallel	5.14	3.49	$3.91 \cdot 10^{-14}$	1	7.07	12711.47	$2.34 \cdot 10^{-8}$	1

we computed both matrices Q and R explicitly, the illustrated runtimes are averages of 10 code executions and we executed the parallel MGS on all 4 available processors. The parallel algorithm has significantly lower runtimes. In particular, we can see that Algorithm 4 performs very well on the two tall and skinny matrices W^1 and W^2. However, when it comes to small square matrices like W^3 (Hilbert matrix) the sequential algorithm matches almost the performance of the parallelized version. Note that both algorithms are considerably slower than our CGS algorithms.

3.3 Numerical Stability of MGS

In general, MGS provides backward stable solutions [2]. Regarding the loss of orthogonality, Grigori [5] gives the following bound: Assuming $c(m, b)\kappa(W)u < 1$, it holds $||I - Q^TQ||_2 = c(m, b)\kappa(W)u$ with $c(m, b) = O(mb)$. Therefore, the orthogonality error of MGS scales only linearly w.r.t. the condition $\kappa(W)$ and not quadratic as for CGS. Table 2 shows the orthogonality loss as well as the condition $\kappa(Q)$ for sequential and parallel MGS (Algorithms 3 and 4).

In Figure 5, we plot the orthogonality loss of MGS for a sequence of matrices generated by the procedure described in Section 2.3. In the plot on the left, the green line shows $\kappa(W)u$ as a reference. Both, sequential and parallel MGS (Algorithms 3 and 4), match the predicted orthogonality loss. It is noticeable that parallel MGS has a slightly smaller orthogonality loss than the sequential one. In the plot on the right, we can see that the condition of the input matrix $\kappa(W)$ has only a small impact on $\kappa(Q)$.

Finally, Figure 6 shows the evolution of the orthogonality loss $||I - Q^TQ||_2$ as well as the condition of the orthonormal basis Q in each iteration of Algorithms 3 and 4 for our four test matrices. Both algorithms behave similarly. The orthogonality loss of Q is slightly lower than in Figure 3 and the condition $\kappa(Q)$ scales only slowly w.r.t. $\kappa(W)$. This is a massive improvement compared to CGS and confirms the theory as well as our observations from Figure 5.

4 Tall Skinny QR (TSQR) Decomposition

The tall skinny QR (TSQR) decomposition of a matrix W developed by Demmel, Grigori, Hoemmen, and Langou [4] is a communication optimal QR decomposition for matrices with many more rows than columns ($m \gg n$). The basic idea is to use a reduction-like operation on a tree to compute the QR factorization: First, the algorithm scatters $\frac{m}{P} \times n$ row-blocks B of the $m \times n$ matrix W across P processors. Second, the QR decomposition is computed in each local block independently. Third, the processors recombine the R factors within each group of neighboring processors and continue the process by communicating their R factors to the next set of neighbors. For an illustration, see [4]. The major difference between sequential and parallel TSQR is the underlying tree structure which is used for the matrix factorization.

Figure 5: MGS - Orthogonality loss and $\kappa(Q)$ as function of $\kappa(W)$

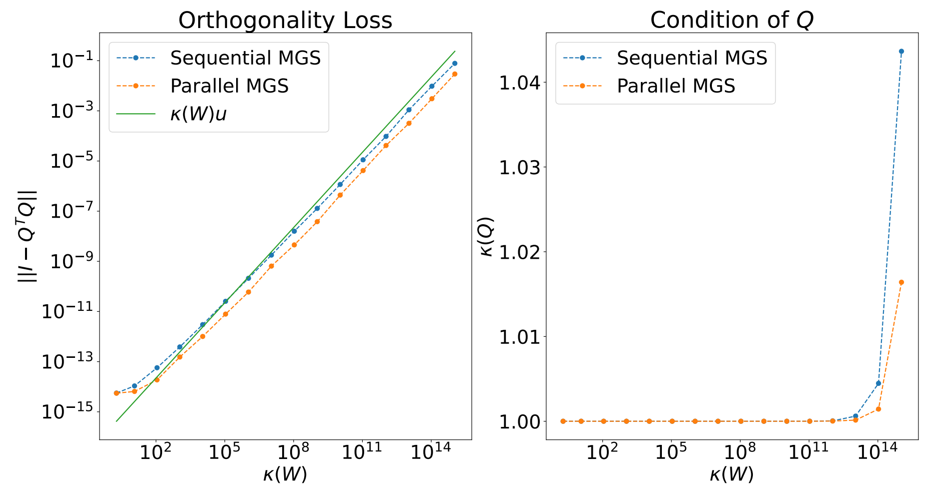

Algorithm 5 Sequential TSQR with implicitly stored Q

```
1: $b = m/P$
2: $B = W[1 : b, :]$
3: for $i = 1$ to $P$ do
4:     if $i > 1$ then
5:         $B = \begin{pmatrix} R \\ W[(i-1)\cdot b:i\cdot b,:] \end{pmatrix}$
6:     end if
7:     $Q_i, R = \text{QR}(B)$
8: end for
9: return $R$
```

4.1 Sequential TSQR

Sequential TSQR uses a *flat tree* or *linear chain* for the factorization process. As described above, we first divide the input matrix W into row-blocks $B_i \in \mathbb{R}^{\frac{m}{P} \times n}$ with $i \in [P]$ and compute the QR decomposition of B_1. Then, we combine the factor R_1 with B_2 by *stacking* the two matrices on top of each other and compute the QR decomposition of $\begin{pmatrix} R_1 \\ B_2 \end{pmatrix}$. We continue this process until we run out of matrices B_i. The R factor of the final iteration is the R factor of the QR decomposition of W. The Q factor can be retrieved by computing a specific matrix product of the local Q factors obtained in each iteration (for details see [4]). However, in practice, it is useful to store the local Q factors implicitly, analogous to using the Householder vectors computed by Householder QR as an implicit representation of the Q factor. Algorithm 5 illustrates the described procedure.

4.2 Parallel TSQR

Parallel TSQR fits into the same general framework as the sequential TSQR decomposition. The difference is that we use a *binary tree* instead of a flat tree. In Algorithm 6, we first divide the input matrix W into row-blocks $B_{p_i,0} \in \mathbb{R}^{\frac{m}{P} \times n}$ with $p_i \in [P]$ and 0 indicating the bottom tree level. Next, we compute the QR decomposition of all local blocks $B_{p_i,0}$ in parallel and group the resulting $R_{p_i,0}$ factors by stacking successive pairs $\begin{pmatrix} R_{p_i,0} \\ R_{p_{i+1},0} \end{pmatrix}$. In the next iteration, we compute the QR decomposition of these pairs on $P/2$ processors and recombine again. We perform iterations until there is only one R factor left. This is the root of the binary tree and the R factor of the QR decomposition of W. The final Q can be computed explicitly based on the local $Q_{p_i,j}$ distributed across the processors as shown in our Python implementation in Listing **??**. We simply traverse the binary tree backward, splitting the matrix $Q_{p_i,j}$ into an upper and lower half $Q_{p_i,j} = \begin{pmatrix} Q_{p_i u,j} \\ Q_{p_i l,j} \end{pmatrix}$ at each tree level j. The lower half $Q_{p_i l,j}$ is sent to a neighboring processor p_k and the two matrix-matrix

Figure 6: Numerical Analysis of MGS

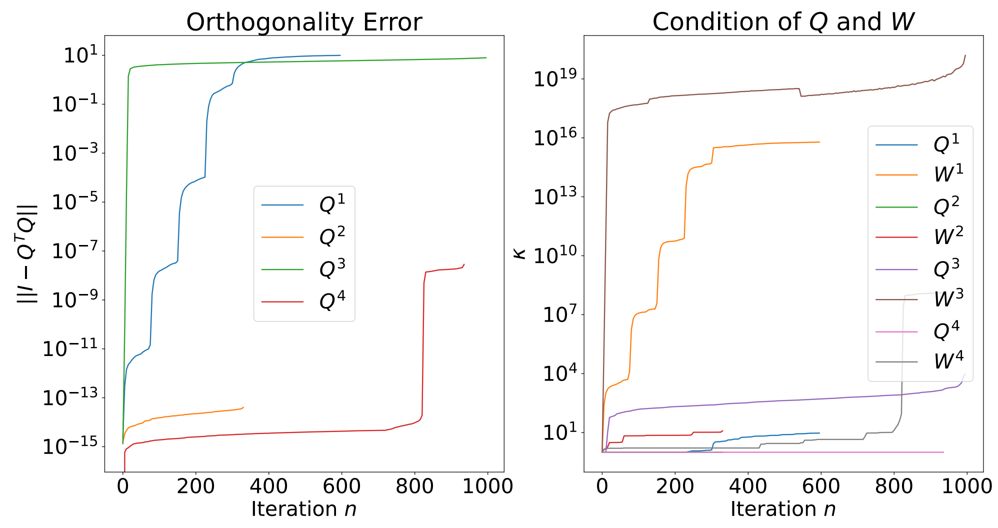

(a) Sequential MGS

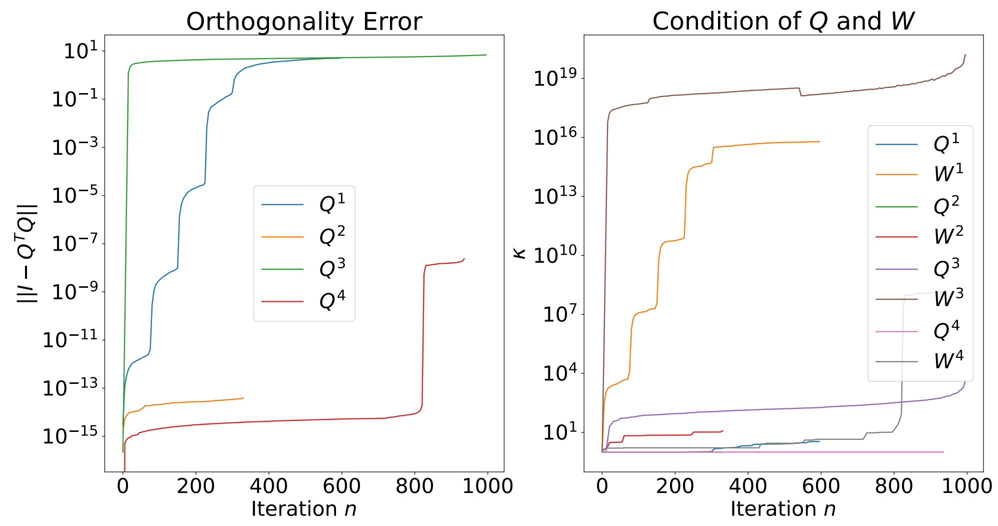

(b) Parallel MGS

products $Q_{p_i,j-1} \cdot Q_{p_i u,j}$, $Q_{p_k,j-1} \cdot Q_{p_i l,j}$ are computed in parallel. At the bottom tree level, the local Q products are gathered together and the resulting matrix is the Q factor of the QR decomposition of W. This backward traversal is advantageous compared to computing Q in the same iterations as R because of reduced matrix dimensions. $Q_{i,0}$ has dimensions $\frac{m}{P} \times n$ and $Q_{i,j}$ for $j > 1$ has dimensions $2n \times n$. If we started computing Q at the tree leaves, we would have to compute the matrix product of a $\frac{m}{P} \times n$ and a $n \times n$ matrix in each iteration. In contrast, if we start computing Q at the tree root, we only need to calculate the matrix product two $n \times n$ matrices until the very last iteration (in which we have to face a matrix product of a $\frac{m}{P} \times n$ and a $n \times n$ matrix).

In practice, however, it is preferable to store Q implicitly. Note that a binary tree and therefore our algorithm works only for the number of processes P being a power of 2. Finally, it holds $\#$ messages $\doteq \log(P)$ for parallel TSQR and the number of messages does in particular not depend on the matrix size. Therefore, the algorithm scales very well for large matrices.

Algorithm 6 Parallel TSQR with implicitly stored Q

```
1: MPI.Scatterv($W$, $B$, root = 0)
2: $P_{label} = rank$
3: $Q_0, R = \text{QR}(B)$
4: for $i = 1$ to $\log_2(P)$ do
5:     if $P_{label} \mod 2 == 0$ then
6:         MPI.Recv($R_{temp}$, source = $rank + i$)
7:         $R = \binom{R}{R_{temp}}$
8:         $Q_i, R = \text{QR}(R)$
9:     else
10:        MPI.Send($R$, dest = $rank - i$)
11:        BREAK
12:    end if
13:    $P_{label} = \lfloor (P_{label} + 1)/2 \rfloor$
14: end for
15: return $Q, R$
```

Figure 7: Runtime of TSQR Algorithms

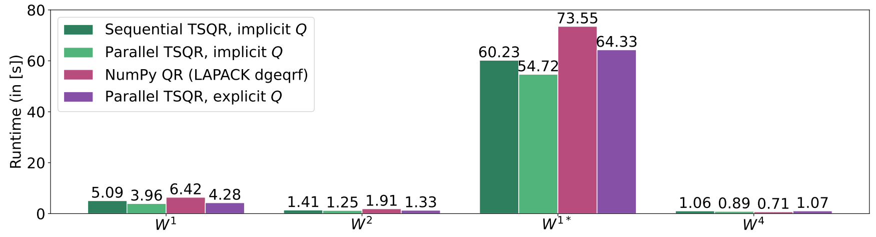

4.3 Performance Evaluation of TSQR

In this section, we compare the runtime of sequential and parallel TSQR. Unfortunately, we cannot use the Hilbert matrix W^3 for testing TSQR because it requires per construction $m \geq Pn$. Instead of W^3 we reuse W^1 but with dimensions $m = 300.000, n = 900$ and call the matrix W^{1^*}. To get an impression of the effect of an implicitly stored Q, we present the runtimes of both, implicitly and explicitly computed Q, for parallel TSQR. Furthermore, we use the NumPy in-built function *numpy.linalg.qr* as a subroutine in our Python implementations of the TSQR algorithms. Therefore, we will additionally present the runtimes of this function. As before, we limited the threads available to the BLAS library to 1. This means that the NumPy QR will work only sequentially. Figure 7 illustrates our results for W^1, W^2, W^{1^*} and W^4. The shown runtimes have been obtained as averages of 10 code executions and we used all 4 available processors for parallel TSQR. From the plot, it becomes clear that both TSQR algorithms outperform NumPy QR on the tall and skinny matrices W^1, W^2, W^{1^*}. When it comes to matrix W^4 which has "only" 4 times as many rows as columns, the NumPy QR is the best choice. Furthermore, the implicit and explicit computation of Q might not have a huge performance impact for smaller matrices, but when it comes to W^{1^*}, the implicit storage reduces the execution time by almost 15%.

4.4 Numerical Stability of TSQR

As already mentioned, we use the NumPy in-built function *numpy.linalg.qr* as a subroutine for our TSQR algorithms. This function is an interface to the LAPACK routine *dgeqrf* which uses Householder QR. Similar to MGS, Householder QR gives backward stable solutions [2]. Moreover, Householder QR is unconditionally stable [4], i.e. the computed Q factors are always orthogonal to machine precision independent of the input matrix W: $||I - Q^TQ||_2 = O(u)$. Our TSQR algorithms are composed of multiple QR decompositions. Since these factorizations are unconditionally stable, sequential and parallel TSQR are also unconditionally stable. The orthogonality loss as well as the condition $\kappa(Q)$ for our test matrices W^1, W^2, W^{1^*} and W^4 can be found in Table 3. In Figure 8, we plot the orthogonality loss and $\kappa(Q)$ for the sequence of test matrices generated by the procedure described in Section 2.3. As expected, NumPy QR and both TSQR algorithms produce results that

Table 3: Orthogonality Error $||I - Q^TQ||_2$ of TSQR (loss scaled by 10^{-14})

Algorithm	$\mathbf{W}^1$		$\mathbf{W}^2$		$\mathbf{W}^{1^*}$		$\mathbf{W}^4$	
	loss	$\kappa(Q)$	loss	$\kappa(Q)$	loss	$\kappa(Q)$	loss	$\kappa(Q)$
Sequential	1.39	1	1.39	1	3.05	1	1.41	1
Parallel	1.35	1	1.45	1	2.99	1	1.38	1
NumPy QR	1.27	1	1.33	1	3.16	1	1.01	1

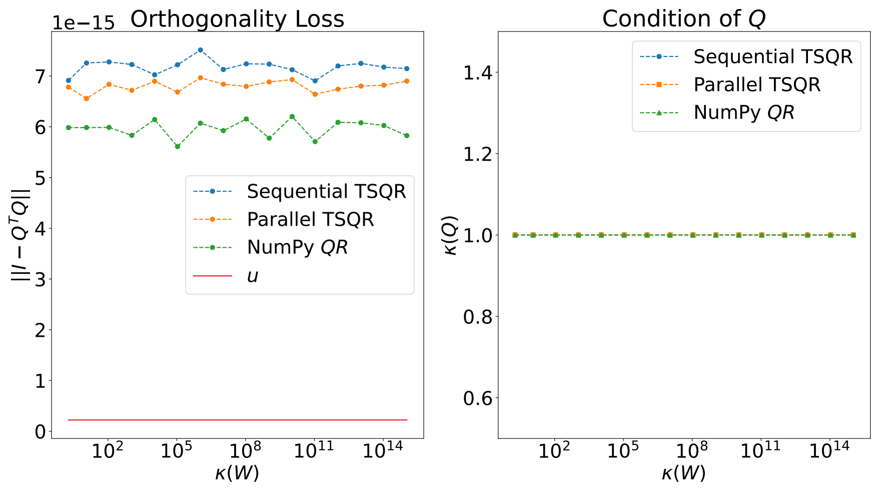

Figure 8: TSQR - Orthogonality loss and $\kappa(Q)$ as function of $\kappa(W)$

are orthogonal to the machine precision independent of the given matrix. Furthermore, $\kappa(Q)$ is 1 for all matrices.

5 Conclusion

To conclude, TSQR is the best choice for parallelizing the QR decomposition of tall and skinny matrices. In contrast to CGS and MGS, it is unconditionally stable and the number of required messages scales independently of the matrix size (# messages $\doteq \log(P)$). As the theory predicted, CGS was so unstable in our experiments that it is not useful in practice. MGS is backward stable but the orthogonality error still scales linearly with the condition of the matrix. Although CGS and MGS require the same amount of floating point operations, MGS is much slower in practice than CGS. An advantage of CGS and MGS is that the already computed vectors in each iteration form an orthonormal basis. In particular, each vector q_i can be obtained after the i-th iteration. In contrast, when using TSQR or Householder QR one has to wait until the completion of the algorithm to obtain any orthonormal vector. The amount of messages sent while executing CGS or MGS scales linearly with the number of columns of the input matrix and the corresponding lower bound for both algorithms is $2n \log(P)$ [4].

References

[1] Oleg Balabanov and Laura Grigori. Randomized gram-schmidt process with application to gmres, 2022.

[2] Folkmar Bornemann. *Numerische lineare Algebra*. Springer Spektrum Wiesbaden, 2018. ISBN 978-3-658-24431-6. doi: https://doi.org/10.1007/978-3-658-24431-6.

[3] Timothy A. Davis and Yifan Hu. The university of florida sparse matrix collection. *ACM Trans. Math. Softw.*, 38(1), 12 2011. ISSN 0098-3500. doi: 10.1145/2049662.2049663. URL `https://doi.org/10.1145/2049662.2049663`.

[4] James Demmel, Laura Grigori, Mark Hoemmen, and Julien Langou. Communication-optimal parallel and sequential qr and lu factorizations: theory and practice, 2008.

[5] Laura Grigori. Communication avoiding qr factorization and orthogonalization of a set of vectors. Lecture notes for the course "HPC for numerical methods and data analysis" at EPFL, 2023.

[6] Gudula Rünger and Michael Schwind. Comparison of different parallel modified gram-schmidt algorithms. volume 3648, pages 826–836, 08 2005. ISBN 978-3-540-28700-1. doi: 10.1007/11549468_90.

[7] Katarzyna Swirydowicz, Julien Langou, Shreyas Ananthan, Ulrike Yang, and Stephen Thomas. Low synchronization gram–schmidt and generalized minimal residual algorithms. *Numerical Linear Algebra with Applications*, 28(2), 10 2020. ISSN 1070-5325. doi: 10.1002/nla.2343. URL `https://www.osti.gov/biblio/1710196`.